

# Crystallization Kinematics and Dielectric Behavior of (Ba,Sr)TiO<sub>3</sub> Borosilicate Glass Ceramics

Avadhesh Kumar Yadav<sup>1</sup>, Chandkiram Gautam<sup>1\*</sup>, Prabhakar Singh<sup>2</sup>

<sup>1</sup>Department of Physics, University of Lucknow, Lucknow, India; <sup>2</sup>Department of Applied Physics, Institute of Technology, Banaras Hindu University, Varanasi, India.

Email: \*gautam\_ceramic@yahoo.com

Received January 16<sup>th</sup>, 2012; revised March 24<sup>th</sup>, 2012; accepted April 27<sup>th</sup>, 2012

## ABSTRACT

Perovskite [(Ba<sub>0.6</sub>Sr<sub>0.4</sub>)TiO<sub>3</sub>]-[2SiO<sub>2</sub>-B<sub>2</sub>O<sub>3</sub>]-[K<sub>2</sub>O]-La<sub>2</sub>O<sub>3</sub> glass was prepared by conventional melt quench method. The differential thermal analysis (DTA) was performed on glass sample in the temperature range from 100°C to 1000°C by different heating rate to study the crystallization kinematics. The kinetic parameters characterizing the crystallization have been determined using an Arrhenius model. Glass samples were subjected to appropriate heat treatment schedules for their suitable crystallization. X-ray diffraction analysis (XRD) of glass and glass ceramic samples were done to check the amorphous state and crystalline nature. XRD of glass ceramic sample shows the major perovskite phase of BaTiO<sub>3</sub> (BT) along with the formation of secondary phases Ba<sub>2</sub>TiSi<sub>2</sub>O<sub>8</sub> (BTS) and Ba<sub>2</sub>Ti<sub>2</sub>B<sub>2</sub>O<sub>9</sub> (BTB). Scanning electron microscopy (SEM) is also studied to see the morphology of the grains of major and secondary phase formation in BST glass ceramic samples. La<sub>2</sub>O<sub>3</sub> is played an important role to increase the nucleation of the crystallites in the glassy matrix. The addition of La<sub>2</sub>O<sub>3</sub> results in development of well interconnected crystallites formed as major phase of BST. In this paper, we are reporting the crystallization behavior of BST borosilicate glass system and high temperature dielectric characteristics of their glass ceramics.

**Keywords:** BST Glass Ceramics; DTA; Crystallization; XRD; SEM; Dielectric Constant

## 1. Introduction

Glass ceramics are polycrystalline materials produced by high-temperature, controlled nucleation and crystallization of glasses. Glass ceramics have become established as commercially important materials in the fields such as consumer products, vacuum tube envelopes, telescope mirror blanks, radomes for the aerospace industry and protective coating for metals [1]. Glasses are thermodynamically unstable as compared with the isochemical crystals due to glass formation, which was reported by Tammann [2], among others. Their study showed that crystallization processes occur by nucleation and growth and it depends on the temperature and the substance, either step may determine the rate of spontaneous crystallization. Therefore, at least two free energy barriers are involved in the metastability of the supercooled liquid. The first process is the free energy of crystal nucleus formation which is arising primarily because of the melting point of small crystals is lower than that of large crystals. The second barrier is due to impeded molecular motion at the crystal to liquid interface in going from a liquid to a crystal-like position. Extensive studies have

been reported on the crystallization and dielectric behavior of ferroelectric glass ceramics, specifically PbTiO<sub>3</sub> and NaNbO<sub>3</sub> [3]. The paraelectric and ferroelectric phase transition in BaTiO<sub>3</sub> disappears below a critical size [4]. There are some factors that influence the properties of the major crystalline phase in a glass ceramic are the surrounding glass matrix, their crystallization kinetics and nucleation mechanism, particle size and presence of other crystalline phases. Crystallization and properties of BaTiO<sub>3</sub> in the system BaO-TiO<sub>2</sub>-Al<sub>2</sub>O<sub>3</sub>-SiO<sub>2</sub> have been reported [5-8]. BST is a dielectric material with excellent dielectric properties such as high dielectric constant, small dielectric loss, low leakage current, large dielectric breakdown strength. It is thought to be the most promising dielectric material for the memory cell capacitors in dynamic random access memory (DRAM) with very large scale integration (VLSI) [9,10]. BST is the solid solution of BaTiO<sub>3</sub> and SrTiO<sub>3</sub> with effective dielectric properties, which has been used in electronic, electrooptical, optical, acoustic, and microwave devices [11-13]. Doping of La<sub>2</sub>O<sub>3</sub> in [SrO·TiO<sub>2</sub>]-[SiO<sub>2</sub>·B<sub>2</sub>O<sub>3</sub>] influences the crystallization of the glass as well as dielectric properties of the glass ceramic samples in the present system. Dielectric constant of these glass ceramic

\*Corresponding author.

ics is high of the order of thousands unlike that of glass ceramics obtained from glasses without La<sub>2</sub>O<sub>3</sub> and it diffuses into the crystalline phase and make it to semi-conducting during the crystallization of the different glass samples at high temperature [14-16]. The study of glass ceramics system

[(Pb<sub>x</sub>Sr<sub>1-x</sub>)O·TiO<sub>2</sub>]-[2SiO<sub>2</sub>-B<sub>2</sub>O<sub>3</sub>]-[K<sub>2</sub>O]-[BaO]-[La<sub>2</sub>O<sub>3</sub>], shows dispersion of semiconducting perovskite phase in insulating glassy matrix and may lead to space charge polarization around crystal glass interface, imparting high value of effective dielectric constant. These glass ceramics may be used for capacitor applications [17]. Recently, investigated system was crystallization behavior and microstructural analysis of lead and strontium rich (Pb<sub>x</sub>Sr<sub>1-x</sub>)TiO<sub>3</sub> glass ceramics in presence of La<sub>2</sub>O<sub>3</sub>. The doping of La<sub>2</sub>O<sub>3</sub> in the (PbSr)TiO<sub>3</sub> borosilicate glass ceramic system enhances the crystallization and retards the minor phase [18,19].

## 2. Experimental Procedure

The AR grade chemicals BaCO<sub>3</sub> (Himedia 99%), SrCO<sub>3</sub> (Himedia 99%), TiO<sub>2</sub> (Himedia 99%), SiO<sub>2</sub> (Himedia 99.5%), H<sub>3</sub>BO<sub>3</sub> (Himedia 99.8%), K<sub>2</sub>CO<sub>3</sub> (Himedia 99.9%) and La<sub>2</sub>O<sub>3</sub> (Himedia 99.9%) were used for the preparation of glass composition



The appropriate amounts of these ingredients were mixed in a mortar using acetone as a grinding medium. The well mixed and dried powder was transferred in to a high alumina content crucible and then crucible is replaced inside the high temperature SiC programmable electric furnace. The melt was poured into an aluminum mould and pressed by a thick aluminum plate then immediately transferred in to a preheated muffle furnace for annealing at temperature 450°C for 3 hours. DTA was done on the coarse powdered glass samples at heating rate 5°C, 10°C, 15°C, 20°C and 25°C. On the basis of DTA results, various glass samples were subjected regulated heat treatment schedules at 820°C and 853°C with heating rate of 2°C/min for 3 hours soaking time for the crystallization. The crystallized samples were then cooled to room temperature with cooling rate of 5°C/min. The nomenclature of glass ceramic samples includes the code of their parent glass composition followed by heat treatment temperature by a letter "T" for 3 hours heat treatment schedule. XRD of glass ceramic samples were carried out using a Rigaku Miniflex-II X-ray diffractometer using Cu-K $\alpha$  radiation. XRD patterns were compared with standard d-values from JCPDS files for different constituting phases. Glass ceramic samples were polished and etched using a solution of 30% HNO<sub>3</sub> + 20% HF. Gold-Palladium coating were done by sputtering method (Poraton Sc-7640 Sputter) on the etched surface of various glass ce-

ramic samples for SEM. SEM images were recorded by using (model LEO 430 Cambridge Instruments Ltd. UK) to study the morphology of different crystalline phases. For dielectric measurement of glass ceramic samples, both the surfaces of these samples were ground and polished using SiC powders of 100, 600 and 800 mesh to attain the smooth surfaces to get desired thickness of the samples (0.5 to 1 mm). These smooth glass ceramic samples were further polished by emery paper of different grades 1/0, 2/0, 3/0 and 4/0 and thereafter polished by diamond paste with Hifin fluid "OS". The well polished glass samples were electroded by applying the silver paint (Code No. 1337-A, Elteck Corporation, India) on both sides of the specimen and curing at 700°C for 5 minutes. The capacitance, *C*, measurements were made in a well fabricated sample holder using an automated measurement system during heating. The leads from the sample holder were connected to Wayne Kerr 6500 P (high frequency LCR Meter, Frequency: 20 Hz - 5 MHz) through scanner relay boards and HPIB bus, which in turn was connected to a computer and printer. Measurement operational controls and data recording are done through the computer. *C* and dissipation factor, tan  $\delta$ , of the glass ceramic samples were recorded with 60 Hz, 0.1, 10, 100 kHz, 1, 2 and 5 MHz in equal intervals of time during heating in the temperature range 60°C - 700°C. Dielectric constant,  $\epsilon_r$ , was calculated from the measured, *C* using the following equation:

$$\epsilon_r = \frac{C \times d}{\epsilon_0 A} \quad (1)$$

where, *C* is the capacitance in farad,  $\epsilon_0$  is the permittivity of free space ( $8.85 \times 10^{-12}$  F/m), *d* is the thickness (m) and *A* is the area (m<sup>2</sup>) of the samples. The  $\epsilon_r$  and tan  $\delta$ , were plotted as a function of temperature, *T*, at a few selected frequencies to show the variation of  $\epsilon_r$ , with *T*, and frequency of applied electric field. tan $\delta$  was noted directly or calculated by using the following relation:

$$\tan \delta = \frac{G}{\omega C} \quad (2)$$

where  $\omega = 2\pi f$ , *f* is the frequency and *G* is the conductance.

## 3. Results and Discussion

### 3.1. Differential Thermal Analysis (DTA)

The crystallization temperature, *T<sub>c</sub>*, of BST in the glass matrix at different heating rates ( $\phi$ ) was studied through DTA. DTA pattern of glass sample BST5K1L0.4 for different heating rate are shown in **Figure 1**. The heating rate and crystallization temperatures (*T<sub>c</sub>*) of glass sample are listed in **Table 1**. This pattern shows the evolution of crystallization exotherms as a function of heating rate,  $\phi$ ,

for the glass sample. DTA pattern of this glass sample shows two exothermic peaks at 820°C and 853°C with heating rate of 2°C/min. Kinetics of the crystallization of BST glass ceramics were evaluated from the measurements by which the crystallized fraction of BST phase at a given temperature. It is observed from the DTA patterns that  $T_c$  increases with  $\phi$  along with an increase in intensity of the peaks which indicates the activation controlled crystallization. Therefore, the method reported by Kissinger [20-23] was employed to determine the kinetic parameters associated with the crystallization of the BST phase. The Kissinger equation is given as:

$$\ln \frac{\phi}{T_m^2} = \frac{-E_a}{R} \frac{1}{T_m} + \ln \frac{A}{E_a/R} \quad (3)$$

where  $\phi$  is the heating rate,  $E_a$  is the activation energy of crystallization,  $R$  is the universal gas constant,  $A$  is the preexponential frequency factor and  $T_c$  is the crystallization temperature. The curve is plotted  $\ln(\phi/T_c^2)$  versus  $1/T_c$  (**Figure 2**). The slope of this plot gives  $-E_a/R$ . The activation energy,  $E_a$  for crystallization of BST is estimated as 762 kJ/mol, which greater that reported value 705 kJ/mol [24]. This indicates the sluggishness of the crystallization in glass matrix due to 1 mole percent doping of La<sub>2</sub>O<sub>3</sub>. The preexponential frequency factor,  $A$  is determined by yintercept and which is found to be  $1.93 \times 10^{36} \text{ sec}^{-1}$  and the reaction rate constant,  $k$  determined by Arrhenius equation ( $k = Ae^{-E_a/RT}$ ) at temperature 820°C is  $1.932 \text{ sec}^{-1}$ , this indicates that a rapid transition from activated state to crystalline state. Thus La<sub>2</sub>O<sub>3</sub> serves as nucleating agent for the crystallization of the glass. In general, surface and volume crystallization occur in glass ceramics. The dominant nucleation mechanism was determined from the peak profile analysis of crystallization exotherms. If  $\Delta T_{FWHM}$  is the full width at half maximum of the crystallization peak, the crystal growth dimension “ $n$ ” can be estimated, as reported earlier [25], from the relation,

$$n = 2.5 \left( \frac{R}{E_a} \right) \left( \frac{T_m^2}{\Delta T_{FWHM}} \right) \quad (4)$$

The value of  $\Delta T_{FWHM}$  is estimated from **Figure 1** as 20 at 835°C and “ $n$ ” come out to be 1.7. A value of  $n = 1$  indicates dominant surface nucleation and  $n = 3$  indicates dominant internal nucleation. Thus, simultaneous surface and internal crystallization occurs from the glass matrix [26-28].

### 3.2. X-Ray Diffraction Analysis

XRD patterns of BST borosilicate glass and glass ceramic samples are shown in **Figure 3**. The XRD pattern of glass sample BST5K1L0.4 shows diffuse pattern and

**Table 1. Heating rate and crystallization temperatures ( $T_c$ ) of glass sample.**

Heating Rate (°C/minute)	Crystallization Temperature ( $T_c$ )	
	$T_{c1}$	$T_{c2}$
5	820	853
10	827	860
15	835	868
20	841	874
25	848	881

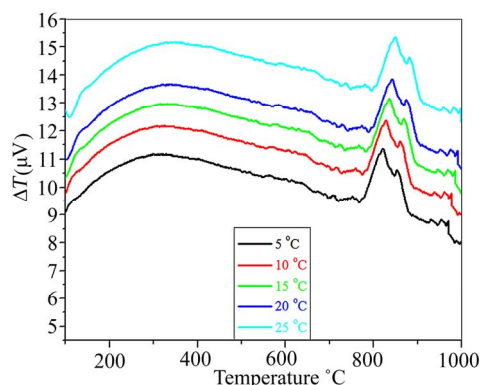


**Figure 1. DTA pattern of glass samples with different heating rate.**

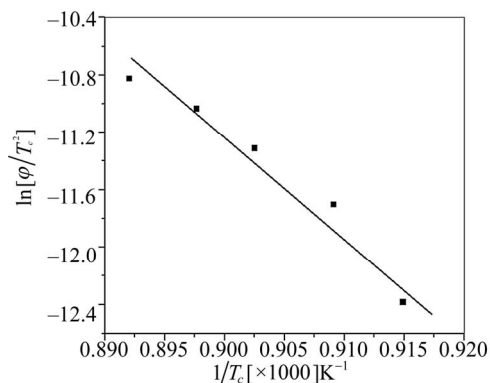


**Figure 2. Plot of  $\ln(\phi/T_c^2)$  versus  $1/T_c$ .**

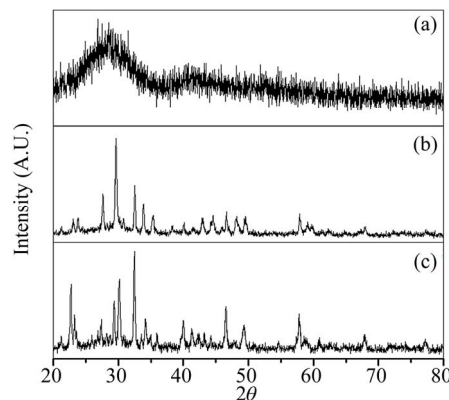


**Figure 3. X-ray diffraction patterns of glass and glass ceramic samples (a) BST5K1L0.4; (b) BST5K1L0.4T820; and (c) BST5K1L0.4T853.**

no clear peak is observed (**Figure 3(a)**) which indicates amorphous nature of the glass. XRD patterns of glass ceramic samples show BST is the major crystalline phase whereas BTS and BTB are the secondary phases. **Figures 3(b)** and **(c)** depicts the XRD patterns of BST5K1L0.4T820 and BST5K1L0.4T853. The crystallization at low temperature peak,  $T_{c1}$ , corresponds to crystallization of perovskite major phase of BST, while the high temperature peak,  $T_{c2}$ , corresponds to the crystallization of secondary phase. The crystallite size was calculated by using Scherer formula [29].

$$\text{Crystallite size } D_p = \frac{K\lambda}{\beta \cos \theta} \quad (5)$$

where,  $K$  is the shape factor (0.94),  $\lambda$  is wavelength of Cu-K $\alpha$  line (1.54 Å) and  $\beta$  is full width at half maximum. The crystallite size of glass ceramic sample BST5K1L0.4T853 is 35.6 nm. This sample shows the cubic crystal structure and having the value of lattice parameters,  $a = b = c = 3.9$  Å [30].

### 3.3. Scanning Electron Microscopic Analysis

SEM of different glass ceramic samples BST5K1L0.4T820 and BST5K1L0.4S853 are shown in **Figures 4(a)** and **(b)**. **Figure 4(a)** shows randomly agglomerated crystallites of major phase of BST with some residual glassy phase. **Figure 4(b)** shows well interconnect grains of major phase of BST and secondary phase formations are also present as BTS and BTB. It is also confirmed by their XRD pattern. The coexistence of both coarse as well as fine grains are also observed in these micrographs. Well developed and interconnected grains of major phase of BST are distributed inside the micrographs. The grain size is 667 nm were observed for glass ceramic sample BST5K1L0.4T853 while for micrograph of glass ceramic sample BST5K1L0.4T820 is 500 nm. The crystal growth of the crystallites is not perfect and uniform. It is concluded that the heat treatment schedule at 853°C is not suitable for good crystallization in comparison to heat treatment schedule 820°C.

### 3.4. Dielectric Behavior

Dielectric constant,  $\epsilon_r$ , and dissipation factor  $\tan\delta$ , were measured as a function of temperature within the temperature range 60°C to 650°C at a few selected frequencies such as 60 Hz, 0.1, 10, 100 KHz, 1, 2 and 5 MHz for the glass ceramic samples BST5K1L0.4T820 and BST5K1L0.4T853. **Figures 5** and **6** show the dielectric constant and dissipation factor ( $\tan\delta$ ) versus temperature. This shows  $\epsilon_r$ , and  $\tan\delta$  remains constant up to 300°C and thereafter both increases with increasing temperature.  $\epsilon_r$ , and  $\tan\delta$  are all most independent with temperature at

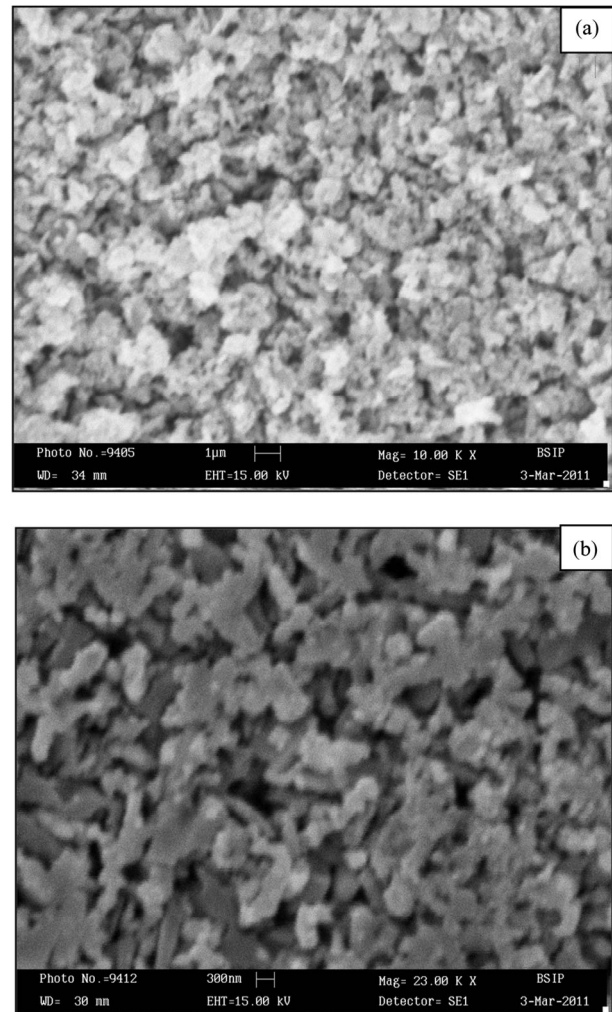


**Figure 4.** Scanning electron micrographs of glass ceramic sample (a) BST5K1L0.4T820 and (b) BST5K1L0.4 T853.

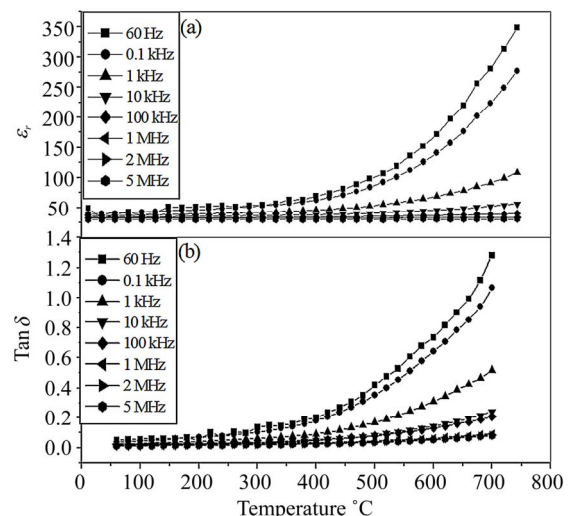


**Figure 5.** Variation of (a) dielectric constant,  $\epsilon_r$  and (b) Dissipation factor,  $\tan\delta$  with temperature at different frequencies for the glass ceramic sample BST5K1L0.4T820.



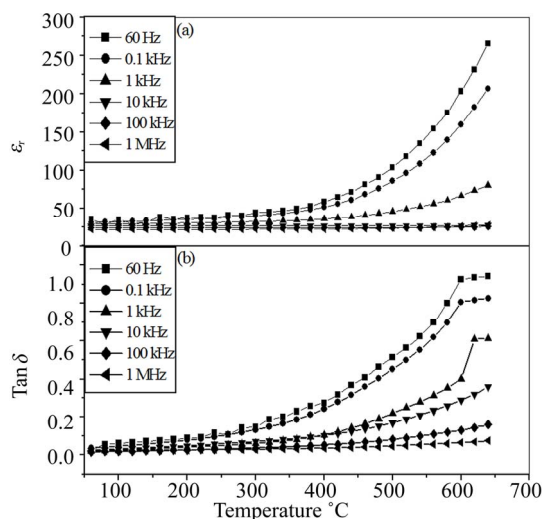


**Figure 6.** Variation of (a) dielectric constant,  $\epsilon_r$  and (b) Dissipation factor,  $\tan\delta$  with temperature at different frequencies for the glass ceramic sample BST5K1L0.4T853.

higher frequencies 100 kHz, 1 MHz, 2 MHz and 5 MHz while it increases at lower frequencies, 60 Hz and 0.1 kHz. The value of  $\epsilon_r$ , at 650°C, is found to be 350 at 60 Hz for glass ceramic sample BST5K1L0.4T820 while its value for glass ceramic sample BST5K1L0.4T853 is found to be 266. This high value of  $\epsilon_r$  is occurring due to these reasons: 1) Glass ceramic sample crystallized at 820°C shows better crystallization in comparison to glass crystallized at 853°C, which also confirmed from the XRD analysis as well as SEM images; 2) Addition effects of 1 mole% donor dopant La<sub>2</sub>O<sub>3</sub>. During the crystallization of glasses La<sub>2</sub>O<sub>3</sub> to stuck with perovskite BST crystalline phase and makes the semiconducting nature to the glass ceramic samples; and 3) Crystallization temperature is one of the important parameters which are described in the part of the DTA results. A conductivity difference is produce between semiconducting crystalline phase of BST and residual glass interface. Therefore, due to this conductivity difference the interfacial polarization is produced, along with the application of the electric field on the glass ceramic samples. Eventually the addition of donar dopant La<sub>2</sub>O<sub>3</sub> acts as a nucleating agent for better crystallization of the glass samples.

#### 4. Conclusion

It is concluded as: 1) Bulk transparent glass of BST borosilicate was prepared; 2) The sluggish crystallization is obtained in the glassy matrix due to addition of 1 mole% of La<sub>2</sub>O<sub>3</sub>; 3) A rapid transition was found from activated state to crystalline state of glass sample; 4) XRD patterns of these glass ceramic samples confirmed the major perovskite phase of BaTiO<sub>3</sub> along with secondary phases of Ba<sub>2</sub>TiSi<sub>2</sub>O<sub>8</sub> and Ba<sub>2</sub>Ti<sub>2</sub>B<sub>2</sub>O<sub>9</sub>; 5) High

value of  $\epsilon_r$  is attributed to interfacial polarization; 6) La<sub>2</sub>O<sub>3</sub> serves as nucleating agent for the crystallization of the glass sample.

#### 5. Acknowledgements

The authors are gratefully acknowledged to the University Grant Commission (UGC), New Delhi, (India) for financial support under major research project F. No. 37-439/2009 (SR).

#### REFERENCES

- [1] P. W. McMillan, "Glass Ceramics," Academic Press, New York, 1979.
- [2] G. Tammann, "The States of Aggregation," Van Nostrand, New York, 1925.
- [3] T. Kokubo and M. Tashiro, "Dielectric Properties of Fine-Grained PbTiO<sub>3</sub> Crystals Precipitated in a Glass," *Journal of Non-Crystalline Solids*, Vol. 13, No. 2, 1974, pp. 328-340.
- [4] C. Estournes, T. Lutz, J. Happich, T. Quaranta, P. Wissler and J. L. Guille, "Nickel Nanoparticles in Silica Gel: Preparation and Magnetic Properties," *Journal of Magnetism and Magnetic Materials*, Vol. 173, No. 1-2, 1997, pp. 83-92. doi:10.1016/S0304-8853(97)00144-3
- [5] K. Kageyama and J. Takahashi, "Tunable Microwave Properties of Barium Titanate-Based Ferroelectric Glassceramics," *Journal of the American Ceramic Society*, Vol. 87, No. 8, 2004, pp. 1602-1605. doi:10.1111/j.1551-2916.2004.01602.x
- [6] K. Oda, T. Yoshino and K. O. Oka, "Preparation and Dielectric Properties of (Ba,Sr)TiO<sub>3</sub>-Al<sub>2</sub>O<sub>3</sub>-SiO<sub>2</sub> Glassceramics," *Memoirs of the School of Engineering Okayama University*, Vol. 17, 1983, pp. 97-105.
- [7] A. Herczog, "Microcrystalline BaTiO<sub>3</sub> by Crystallization from Glass," *Journal of the American Ceramic Society*, Vol. 47, No. 3, 1964, pp. 107-116. doi:10.1111/j.1151-2916.1964.tb14366.x
- [8] D. McCauley, R. E. Newnham and C. A. Randall, "Intrinsic Size Effects in a Barium Titanate Glass-Ceramic," *Journal of the American Ceramic Society*, Vol. 81, No. 4, 1998, pp. 979-987. doi:10.1111/j.1151-2916.1998.tb02435.x
- [9] H. F. Cheng, "Structural and Optical Properties of Laser Deposited Ferroelectric (Sr<sub>0.2</sub>Ba<sub>0.8</sub>)TiO<sub>3</sub> Thin Films," *Journal of Applied Physics*, Vol. 79, No. 10, 1996, pp. 7965-7971. doi:10.1063/1.362346
- [10] D. M. Tahan, A. Safari and L. C. Klein, "Synthesis and Processing Characteristics of Ba<sub>0.65</sub>Sr<sub>0.35</sub>TiO<sub>3</sub> Powders from Catecholate Precursors," *Journal of the American Ceramic Society*, Vol. 79, No. 6, 1996, pp. 1593-1598. doi:10.1111/j.1151-2916.1996.tb08769.x
- [11] O. P. Thakur, C. Prakash and D. Agrawal, "Dielectric Behavior of Ba<sub>0.95</sub>Sr<sub>0.05</sub>TiO<sub>3</sub> Ceramics Sintered by Microwave," *Materials Science and Engineering: B*, Vol. 96, No. 3, 2002, pp. 221-225.

- [doi:10.1016/S0921-5107\(02\)00159-9](https://doi.org/10.1016/S0921-5107(02)00159-9)
- [12] N. J. Ali and S. J. Milne, "Synthesis and Processing Characteristics of Ba<sub>0.65</sub>Sr<sub>0.35</sub>TiO<sub>3</sub> Powders from Catecholate Precursors," *Journal of the American Ceramic Society*, Vol. 76, No. 9, 1993, pp. 2321-2326. [doi:10.1111/j.1151-2916.1993.tb07771.x](https://doi.org/10.1111/j.1151-2916.1993.tb07771.x)
- [13] J. W. Liou and B. S. Chiou, "Effect of Direct-Current Biasing on the Dielectric Properties of Barium Strontium Titanate," *Journal of the American Ceramic Society*, Vol. 80, No. 12, 1997, pp. 3093-3099. [doi:10.1111/j.1151-2916.1997.tb03237.x](https://doi.org/10.1111/j.1151-2916.1997.tb03237.x)
- [14] O. P. Thakur, "Crystallization, Microstructure and Dielectric Behavior of Strontium Titanate Borosilicate Glass Ceramics with Some Additives," Ph.D. Thesis, Banaras Hindu University, Varanasi, 1997.
- [15] C. R. Gautam, D. Kumar, O. Parkash, O. P. Thakur and C. Prakash, "Dielectric Behavior in the Glass Ceramic System [(Pb<sub>1-x</sub>Sr<sub>x</sub>)O·TiO<sub>2</sub>]-[2SiO<sub>2</sub>·B<sub>2</sub>O<sub>3</sub>]-[7BaO]-[3K<sub>2</sub>O] with Addition of La<sub>2</sub>O<sub>3</sub> (0.0 ≤ x ≤ 0.5)," *International Symposium of Research Students on Material Science and Engineering*, Chennai, 20-22 December 2004, pp. 1-11.
- [16] O. P. Thakur, D. Kumar, O. Parkash and L. Pandey, "Crystallization, Microstructure Development and Dielectric Behaviour of Glass Ceramics in the system [SrO·TiO<sub>2</sub>]-[2SiO<sub>2</sub>·B<sub>2</sub>O<sub>3</sub>]-La<sub>2</sub>O<sub>3</sub>," *Journal of Materials Science*, Vol. 37, No. 12, 2002, pp. 2597-2606. [doi:10.1023/A:1015476631462](https://doi.org/10.1023/A:1015476631462)
- [17] D. Kumar, C. R. Gautam and O. Parkash, "Preparation and Dielectric Characterization of Ferroelectric (Pb<sub>x</sub>Sr<sub>1-x</sub>)TiO<sub>3</sub> Glass Ceramics Doped with La<sub>2</sub>O<sub>3</sub>," *Applied Physics Letters*, Vol. 89, No. 11, 2006, pp.12908-12910.
- [18] C. R. Gautam, D. Kumar and O. Parkash, "Crystallization Behavior and Microstructural Analysis of Strontium Rich (Pb<sub>x</sub>Sr<sub>1-x</sub>)TiO<sub>3</sub> Glass Ceramics in Presence of La<sub>2</sub>O<sub>3</sub>," *Advances in Materials Science and Engineering*, Vol. 2011, 2011, pp. 1-9. [doi:10.1155/2011/402376](https://doi.org/10.1155/2011/402376)
- [19] C. R. Gautam, D. Kumar and O. Parkash, "Crystallization Behavior and Microstructural Analysis of Lead-Rich (Pb<sub>x</sub>Sr<sub>1-x</sub>)TiO<sub>3</sub> Glass Ceramics Containing 1 Mole% La<sub>2</sub>O<sub>3</sub>," *Advances in Materials Science and Engineering*, Vol. 2011, 2011, pp. 1-12. [doi:10.1155/2011/402376](https://doi.org/10.1155/2011/402376)
- [20] H. E. Kissinger, "Variation of Peak Temperatures with Heating Rate in Differential Thermal Analysis," *Journal of Research of the National Bureau of Standards*, Vol. 57, No. 4, 1956, pp. 217-221.
- [21] K. Yao, L. Zhang, X. Yao and W. Zhu, "Controlled Crystallisation in Lead Zirconate Titanate Glass-Ceramics Prepared by the Sol-Gel Process," *Journal of the American Ceramic Society*, Vol. 81, No. 6, 1998, pp. 1571-1576. [doi:10.1111/j.1151-2916.1998.tb02518.x](https://doi.org/10.1111/j.1151-2916.1998.tb02518.x)
- [22] V. Kumar, T. A. Asha, K. Sivanandan, P. V. Divya and K. P. Rema, "Sol-Gel Synthesis of PZT-Glass Nanocomposites Using a Simple System and Characterization," *International Journal of Applied Ceramic Technology*, Vol. 3, No. 5, 2006, pp. 345-352. [doi:10.1111/j.1744-7402.2006.02101.x](https://doi.org/10.1111/j.1744-7402.2006.02101.x)
- [23] S.-I. Jang, B.-C. Choi and H. M. Jang, "Phase Formation Kinetics of Xerogel and Electrical Properties of Sol-Gel-Derived Ba<sub>x</sub>Sr<sub>1-x</sub>TiO<sub>3</sub> Thin Films," *Journal of Materials Research*, Vol. 12, No. 5, 1997, pp. 1327-1334. [doi:10.1557/JMR.1997.0181](https://doi.org/10.1557/JMR.1997.0181)
- [24] P. V. Divya and V. Kumar, "Crystallization Studies and Properties of (Ba<sub>1-x</sub>Sr<sub>x</sub>)TiO<sub>3</sub> in Borosilicate Glass," *Journal of the American Ceramic Society*, Vol. 90, No. 2, 2007, pp. 472-476. [doi:10.1111/j.1551-2916.2006.01452.x](https://doi.org/10.1111/j.1551-2916.2006.01452.x)
- [25] J. A. Augis and J. E. Bennet, "Calculation of the Avrami Parameters for Heterogeneous Solid-State Reaction Using a Modification of the Kissinger Method," *Journal of Thermal Analysis and Calorimetry*, Vol. 13, No. 2, 1978, pp. 283-292. [doi:10.1007/BF01912301](https://doi.org/10.1007/BF01912301)
- [26] P. V. Divya, G. Vignesh and V. Kumar, "Crystallization Studies and Dielectric Properties of (Ba<sub>0.7</sub>Sr<sub>0.3</sub>)TiO<sub>3</sub> in Barium Aluminosilicate Glass," *Journal of Physics D: Applied Physics*, Vol. 40, No. 24, 2007, pp. 7804-7810. [doi:10.1088/0022-3727/40/24/032](https://doi.org/10.1088/0022-3727/40/24/032)
- [27] C. S. Ray, Q. Yang, H. Wein-Hai and D. E. Day, "Surface and Internal Crystallization in Glasses as Determined by Differential Thermal Analysis," *Journal of the American Ceramic Society*, Vol. 79, No. 12, 1996, pp. 3155-3160. [doi:10.1111/j.1151-2916.1996.tb08090.x](https://doi.org/10.1111/j.1151-2916.1996.tb08090.x)
- [28] E. P. Gorzkowski, M.-J. Pan, B. A. Bender and C. C. M. Wu, "Effect of Additives on the Crystallization Kinetics of Barium Strontium Titanate Glass-Ceramics," *Journal of the American Ceramic Society*, Vol. 91, No. 4, 2008, pp. 1065-1069. [doi:10.1111/j.1551-2916.2007.02254.x](https://doi.org/10.1111/j.1551-2916.2007.02254.x)
- [29] A. L. Patterson, "The Scherrer Formula for X-Ray Particle Size Determination," *Physical Review*, Vol. 56, No. 10, 1939, pp. 978-982. [doi:10.1103/PhysRev.56.978](https://doi.org/10.1103/PhysRev.56.978)
- [30] H.-L. Wang, "Structure and Dielectric Properties of Perovskite Barium Titanate (BaTiO<sub>3</sub>)," Partial Fulfillment of Course Requirement for MatE 115, San Jose State University, San Jose, 2002.